Structural Study of the Thermal and Photochemical Spin States in the Spin Crossover Complex $[Fe(phen)_2(NCSe)_2]$

Elizabeth J. MacLean,[b] Catherine M. McGrath,[a] Charles J. O'Connor,[d] Claudio Sangregorio,[d] Jon M. W. Seddon,[a] Ekk Sinn,[a] Frank E. Sowrey,[a] Simon J. Teat,[b] Ann E. Terry,[c] Gavin B. M. Vaughan,[c] and Nigel A. Young*[a]

Abstract: The first structural data for $[Fe(phen)_2(NCSe)_2]$ (obtained using the extraction method of sample preparation) in its high-spin, low-spin and LIESST induced metastable high-spin states have been recorded using synchrotron radiation single crystal diffraction. The space group for all of the spin states was found to be *Pbcn*. On cooling from the high-spin state (**HS-1**) at 292 K through the spin crossover at about 235 K to the low-spin state at 100 K (**LS-1**) the iron coordination environment changed to a more regular octahedral geometry and the Fe–N bond lengths decreased by 0.216 and 0.196 Å (Fe–N(phen)) and 0.147 Å (Fe–N(CSe)). When the low-spin state was illuminated with visible light at about 26 K, the structure of this LIESST induced metastable high-spin state (**HS-2**) was very similar to that of **HS-1** with regards to the Fe–phen bond lengths, but there were some differences in the bond lengths in the Fe–NCSe unit between **HS-1** and **HS-2**. When **HS-2** was warmed in the dark to 50 K, the resultant low-spin state (**LS-2**) had an essentially identical structure to **LS-1**. In all spin states, all of the shortest intermolecular contacts (in terms of van der Waals radii) involved the NCSe ligand, which may be important in describing the cooperativity in the solid state. The quality of the samples was confirmed by magnetic susceptibility and IR measurements.

Keywords: iron · LIESST · 1,10-phenanthroline · spin crossover · X-ray crystallography

Introduction

Among the octahedral transition metal complexes with a d^4, d^5, d^6 or d^7 electronic configuration which undergo a temperature or pressure induced spin crossover, those involving Fe^{II} and N-donor ligands are probably the most studied.[1, 2] Complexes of bidentate N-donor ligands such as 1,10-phenanthroline (phen) are often regarded as prototypical as the first evidence of a high-spin ($^5T_2$) to low-spin ($^1A_1$) equilibrium for Fe^{II} was demonstrated for $[Fe(phen)_2(NCS)_2]$ and $[Fe(phen)_2(NCSe)_2]$ in 1966.[3] Following on from the serendipitous discovery[4] that at sufficiently low temperatures visible light can convert a low-spin ground state into a metastable high-spin excited state, it became clear that stimuli other than T or P could be used to induce spin-state transitions. The process involving visible light is usually known as light-induced excited spin state trapping (LIESST),[2, 5, 6] although susceptibility of transient electron paramagnetic states (STEPS) has also been used.[7] It is now known that both LIESST and reverse-LIESST (photo-transformation of the metastable state back to the ground state) may in principle be observed for all iron(II) complexes exhibiting a thermal spin crossover. However, the lifetime of the light-induced metastable state is dependent on: the ligand field strength; differences in the metal–ligand bond lengths in the two states; and the extent of cooperativity between the metal centres.[6] In addition to visible light, it has also been shown that nuclear decay during Mössbauer emission spectroscopy (nuclear decay induced excited spin state trapping (NIESST)[8]) and soft X-rays (soft X-ray induced excited spin state trapping (SOXIESST)[9]) can also result in the population of metastable high-spin states at low temperatures. As a result of this ability to change spin state

[a] Dr. N. A. Young, Dr. C. M. McGrath, J. M. W. Seddon, Prof. E. Sinn,[+] Dr. F. E. Sowrey
Department of Chemistry, The University of Hull
Kingston upon Hull, HU6 7RX (UK)
Fax: (+44) 1482 466410
E-mail: n.a.young@hull.ac.uk

[b] Dr. E. J. MacLean, Dr. S. J. Teat
CLRC Daresbury Laboratory, Daresbury, Warrington
Cheshire, WA4 4AD (UK)

[c] Dr. A. E. Terry, Dr. G. B. M. Vaughan
European Synchrotron Radiation Facility
38043 Grenoble (France)

[d] Prof. C. J. O'Connor, Dr. C. Sangregorio
Advanced Materials Research Institute
Department of Chemistry, University of New Orleans
New Orleans, LA 70148 (USA)

[+] Present address:
Department of Chemistry, University of Missouri-Rolla
Rolla, MO 65409-0010 (USA)

DOI: 10.1002/chem.200304865

with temperature, pressure or photons, spin-crossover compounds are widely studied with potential uses as data storage media, display devices or sensors.[10] Whilst the IR and Mössbauer spectroscopic fingerprints and magnetic susceptibilities of the LIESST induced states have been observed since their original discovery, the structures of the LIESST states have remained more elusive. EXAFS has been used,[11, 12] but it is only very recently that single crystal X-ray diffraction data have been obtained for the LIESST metastable high-spin states in [Fe(propyltetrazole)$_6$](BF$_4$)$_2$],[13] [Fe(methyltetrazole)$_6$](BF$_4$)$_2$],[14] [Fe(phen)$_2$(NCS)$_2$],[15] and [Fe(2,6-di(pyrazol-1-yl)pyridine)$_2$](BF$_4$)$_2$.[16] It is clearly important to know how the LIESST induced metastable high-spin state (usually denoted **HS-2**) is different to the ground high-spin state (usually indicated **HS-1**) and that is the purpose of this investigation.

Whilst [Fe(phen)$_2$(NCS)$_2$] is regarded as one of the prototypical spin crossover compounds, and the abrupt spin crossover near 175 K has been investigated in great detail using a wide range of techniques,[17] the spin crossover at ≈235 K in the selenocyanate analogue, [Fe(phen)$_2$(NCSe)$_2$], has been much less studied despite its magnetic behaviour being reported in the same initial work as that of [Fe(phen)$_2$(NCS)$_2$].[3, 18, 19] In addition to magnetic susceptibility measurements,[20] [Fe(phen)$_2$(NCSe)$_2$] has been investigated using Mössbauer,[3, 18, 19, 21] IR,[3, 18, 19, 22–25] and electronic absorption spectroscopy;[3, 19] powder X-ray diffraction;[3, 18, 19] heat capacity and calorimetric experiments;[24] ^{1}H NMR spin-lattice relaxation times and linewidths;[26] and soft X-ray absorption spectroscopy.[9] In all cases its behaviour is very similar to that of [Fe(phen)$_2$(NCS)$_2$]. LIESST in [Fe(phen)$_2$(NCSe)$_2$] has been demonstrated using IR data,[25] which indicated a transition temperature of ≈29 K for the thermally driven **HS-2** to **LS-2** transition. There is no high quality structural data (single crystal X-ray or EXAFS) available for [Fe(phen)$_2$(NCSe)$_2$] in any of its spin states. In this paper we present synchrotron radiation single crystal X-ray diffraction data for [Fe(phen)$_2$(NCSe)$_2$] in its high-spin (**HS-1**), low-spin (**LS-1**), metastable high-spin (**HS-2**) and low-spin state (**LS-2**) after relaxation of the LIESST state. This is the first reliable structural data available for this important compound.

Results and Discussion

As it has been shown previously[19, 27] that the spin state behaviour in these compounds is critically dependent on the method of sample preparation, the recommended[21, 23, 24, 26] pyridine Soxhlet extraction method was used,[9] which yielded a good crop of very small crystals. The same batch of these crystals was used for all the experiments described below. It should be noted that the alternative diffusion method of sample preparation usually results in incomplete conversion to the low-spin state at low temperature.

Magnetic susceptibility measurements: The spin-crossover quality of the sample was confirmed by the variable temperature magnetic susceptibility data shown in Figure 1. The very sharp transition from high- to low-spin at ≈234 K, with very little hysteresis between the cooling and heating cycles is in excellent agreement with the previous data for samples prepared by the extraction method as compared to those obtained by diffusion.[3, 18–20] It is instructive to note that the diffraction quality single crystals of [Fe(phen)$_2$(NCSe)$_2$] in this work have been obtained using the *extraction* method with μ_{eff} values for the low temperature data of about 0.5 BM, or $\chi_M T$ values of ≈0.1 cm^{3}mol^{-1}K, indicating complete conversion to the low-spin state. In contrast, the previously reported single crystal data[12, 15, 28–30] for [Fe(phen)$_2$(NCS)$_2$] employed samples prepared using the diffusion method which had μ_{eff} values for the low temperature data of ≈2 BM, or $\chi_M T$ values of ≈0.6 cm^{3}mol^{-1}K; this indicates incomplete conversion to the low-spin state at low temperature with a residual high-spin fraction of ≈16%. This behaviour is well known for these different methods of sample preparation.[12, 31] Therefore, as it has been shown previously that X-ray diffraction data gives an average view of mixed spin state systems,[32] we expect to obtain excellent quality data for both the high- and low-spin state forms of [Fe(phen)$_2$(NCSe)$_2$] from these crystals.

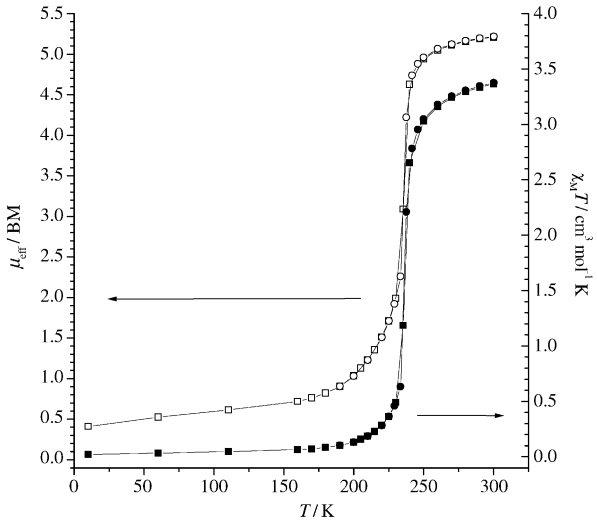

Figure 1. Variable temperature magnetic susceptibility data for [Fe(phen)$_2$(NCSe)$_2$]: Open symbols μ_{eff}, solid symbols $\chi_M T$. Squares represent the cooling cycle, circles the warming cycle.

Infrared studies: In order to confirm that this batch of crystals underwent LIESST, a series of variable temperature IR spectra were recorded, and selected ones are shown in Figure 2. The bands at 2072.6 and 2062.9 cm^{-1} in the 292 K spectrum (Figure 2a) are the ν_{NC} modes of high-spin [Fe(phen)$_2$(NCSe)$_2$] and are in excellent agreement with the previous literature values.[22, 25] The broad peak at 2100 cm^{-1} may represent a small low-spin fraction (<5% based on relative areas) which is not unexpected given the magnetic susceptibility data. On cooling (Figure 2b), the characteristic ν_{NC} modes[22] of low-spin [Fe(phen)$_2$(NCSe)$_2$] at 2110.6 and 2104.6 cm^{-1} are clearly evident by 200 K. The spectrum at 75 K (Figure 2c) confirms that the spin transition is essentially

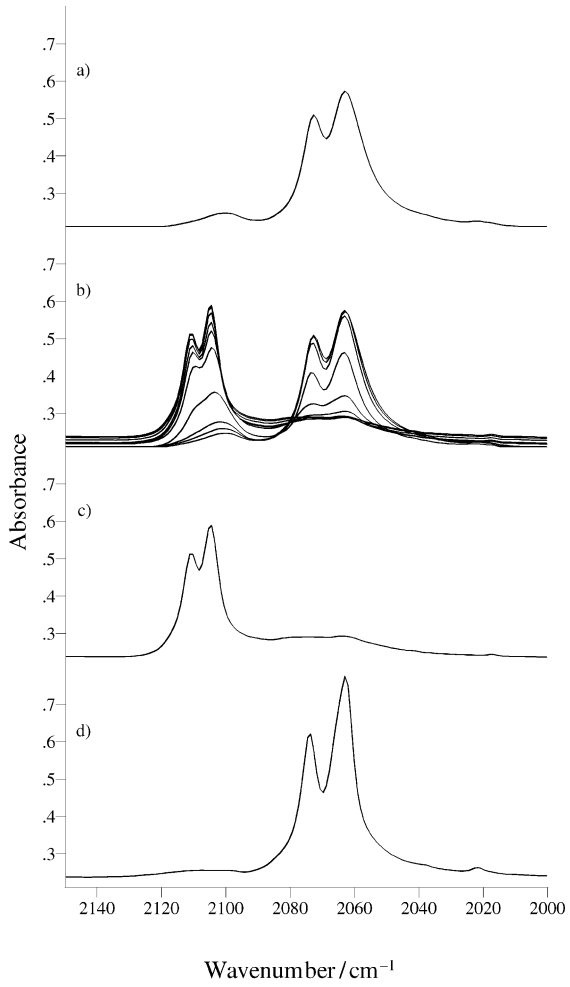

Figure 2. Variable temperature KBr disc IR data for $[Fe(phen)_2(NCSe)_2]$. a) 292 K, b) during cooling (292, 270, 250 K then at 25 K intervals to 75 K), c) at 75 K, d) at 15 K after irradiation with visible light.

complete. The discrepancy in the spin-crossover behaviour in terms of transition temperatures and sharpness between the IR KBr disc data and the magnetic susceptibility data has been noted previously for $[Fe(phen)_2(NCS)_2]$. The origin is thought to be related to the thermal conductivity of the KBr disc in vacuum compared to a He gas environment for the magnetic studies, as well as the grinding and pressure needed for the preparation of the KBr discs.[25, 33, 34] On cooling, the position of the high-spin ν_{NC} modes changes by less than 0.5 cm^{-1}, and once the low-spin modes have become dominant their position is also temperature independent. When the sample was illuminated with visible white light at 75 K only a very small reduction in the low-spin and slight increase in high-spin band intensities was observed. At 65 K, the change was slightly more pronounced but within a minute or so in the dark the sample reverted completely to low-spin. As the temperature was reduced, the proportion of the LIESST induced metastable high-spin state increased, as did its lifetime in the dark. At each temperature there appeared to be a limit to the extent of the formation of the metastable high-spin state, and this only took a few minutes to achieve. This effect was noticed right down to 30 K (at or below the formal limit of many low temperature diffraction devices). Illumination at 15 K (Figure 2d) resulted in only a marginal increase (as compared to the 30 K data) in the intensity of the metastable high-spin bands at 2073.8 and 2062.8 cm^{-1}, and shows that at these temperatures the LIESST process is essentially complete. The position of these bands is very close to the values observed for **HS-1** and it is intriguing that the lower intensity band at 2073.8 cm^{-1} associated with the symmetric mode,[35] shifts by 1.3 cm^{-1}, whereas the asymmetric mode at 2062.8 cm^{-1} is unaffected. The previous IR studies of the **HS-1** and **HS-2** states of $[Fe(phen)_2(NCS)_2]$ contradictory with reported shifts[25] of 4 – 6 cm^{-1}, insignificant shifts,[12] or no reported band positions of the **HS-2** state.[34] There are also some subtle differences in the γ_{CH} region of the IR spectrum with the γ_{CH}(heterocyclic) mode[22] being observed at 725.6 cm^{-1} in both **HS-2** and **HS-1** whilst the γ_{CH}(carbocylic) mode vibrations are found at 847.3 cm^{-1} in **HS-1** and 850.6 cm^{-1} in **HS-2**. In **LS-1** the γ_{CH}(heterocyclic) and γ_{CH}(carbocylic) modes occur at 722.1 and 845.3 cm^{-1}, respectively. There are also some small differences between the unassigned bands[22] at 965 and 765 cm^{-1} in the IR spectra of **HS-1** and **HS-2**. Whilst LIESST in $[Fe(phen)_2NCSe)_2]$ has been monitored previously by IR,[25] neither the spectra nor band positions were given for the **HS-2** state. Even at 15 K, a 5% reduction in the intensity of the metastable high-spin bands was observed over a 25 min period in the dark, but when the lamp was turned back on, the full intensity returned within a minute or so. When the sample was slowly warmed, the metastable state persisted up to $\approx$40 K, but at higher temperatures there was a rapid decrease in the intensity of its characteristic bands. These observations are in excellent agreement with the previous reports[25] and clearly indicate that the $[Fe(phen)_2(NCSe)_2]$ samples prepared in this work fully participate in the LIESST process. During preliminary EXAFS experiments on both $[Fe(phen)_2(NCS)_2]$ and $[Fe(phen)_2(NCSe)_2]$ diluted in polyethylene pressed discs, it was found that the LIESST conversion was only complete if the disc was sufficiently optically transparent to allow the light to penetrate through the whole sample. Therefore, these observations show that it is imperative to use the smallest available crystal at the lowest possible temperature and to keep the crystal illuminated throughout the data collection in order to maintain the highest proportion of the LIESST induced metastable state for the diffraction experiments.

Structural studies using synchrotron radiation single crystal X-ray diffraction: Having demonstrated the high-quality magnetic and optical properties of the crystalline sample of $[Fe(phen)_2(NCSe)_2]$, a single crystal X-ray diffraction study was made of $[Fe(phen)_2(NCSe)_2]$ in its high-spin (**HS-1**), low-spin (**LS-1**), low temperature LIESST induced metastable high-spin (**HS-2**) state and low-spin (**LS-2**) state after relaxation of the LIESST state. The average crystal size was fairly small ($\approx 0.06 \times 0.04 \times 0.02$ mm) and because it was necessary to use the smallest crystals in order to ensure complete light penetration, the synchrotron radiation single crystal X-ray diffraction facilities of both the SRS at Daresbury (station 9.8) and the ESRF in Grenoble (ID11) were utilized.

The high-spin (293 K) (**HS-1**) and low-spin (100 K) (**LS-1a**) structures of $[Fe(phen)_2(NCSe)_2]$ were determined sequentially using the same crystal at station 9.8 at Daresbury. The structures of the low-spin (45 K) (**LS-1b**), low-temperature (26 K) LIESST induced metastable high-spin state (**HS-2**) and low-spin state at 50 K (**LS-2**) after warming from the LIESST state were also obtained sequentially, but at the ESRF using one crystal for all the experiments, and from the same batch as the Daresbury data. The crystal and refinement details are given in Table 1. Although the ESRF was used for the low-temperature data because of the availability of suitable cryostats, it was not possible to obtain room temperature data at the ESRF due to significant radiation damage resulting in a loss of diffracted intensity after a few tens of minutes. The radiation damage at low temperature was sufficiently slow to enable at least four data sets to be collected on each crystal. The observed room temperature radiation damage is not surprising given the increased brilliance of the ESRF compared with Daresbury, coupled with the previous observation of soft X-ray photochemistry in both $[Fe(phen)_2(NCS)_2]$ and $[Fe(phen)_2(NCSe)_2]$.[9]

The space group for all spin states in $[Fe(phen)_2(NCSe)_2]$ was found to be *Pbcn* (Table 1), and the lack of evidence for a significant phase change (i.e., change of space group) between any of the spin states is to be expected from the narrow hysteresis observed in the magnetic susceptibility data.[36] The $[Fe(phen)_2(NCSe)_2]$ molecules (Figure 3) consist of an iron atom surrounded by two isoselenocynate ligands in a mutually *cis* configuration, with two nearly orthogonal bidentate 1,10-phenanthroline (phen) ligands giving an approximately octahedral FeN_6 coordination environment. Although the individual molecules are chiral, the space group is non-chiral as each unit cell contains four molecules, two left-handed and two right-handed. The same space group and similar lattice parameters were also found in the previous X-ray structural determinations for the $[Fe(phen)_2(NCS)_2]$ analogue[12, 15, 28–30] indicating that $[Fe(phen)_2(NCSe)_2]$ and $[Fe(phen)_2(NCS)_2]$ are isostructural. However, due to the excellent quality of the

Table 1. Crystal data and conditions for crystallographic data collection and structure refinement for $[Fe(phen)_2(NCSe)_2]$.

	HS-1	**LS-1a**	**LS-1b**	**HS-2**	**LS-2**
formula	$C_{26}H_{16}FeN_6Se_2$	$C_{26}H_{16}FeN_6Se_2$	$C_{26}H_{16}FeN_6Se_2$	$C_{26}H_{16}FeN_6Se_2$	$C_{26}H_{16}FeN_6Se_2$
M_w	626.22	626.22	626.22	626.22	626.22
crystal system	orthorhombic	orthorhombic	orthorhombic	orthorhombic	orthorhombic
space group	*Pbcn*	*Pbcn*	*Pbcn*	*Pbcn*	*Pbcn*
a [Å]	13.2080(6)	12.8066(18)	12.8242(17)	13.3204(16)	12.8618(16)
b [Å]	10.1828(4)	10.1381(14)	10.137(2)	10.0453(18)	10.1574(16)
c [Å]	17.6681(8)	17.413(2)	17.342(3)	17.391(3)	17.382(3)
α [°]	90	90	90	90	90
β [°]	90	90	90	90	90
γ [°]	90	90	90	90	90
V [Å^3]	2376.26(18)	2260.8(5)	2254.4(7)	2327.0(6)	2270.8(6)
Z	4	4	4	4	4
ρ_{calcd} [g cm^{-3}]	1.750	1.840	1.845	1.787	1.832
absorption coefficient [mm^{-1}]	3.726	3.917	2.078	2.013	2.063
$F(000)$	1232	1232	1232	1232	1232
crystal size [mm]	0.06 × 0.04 × 0.02	0.06 × 0.04 × 0.02	0.05 × 0.03 × 0.02	0.05 × 0.03 × 0.02	0.05 × 0.03 × 0.02
data collection					
λ [Å]	0.6878	0.6878	0.46409	0.46409	0.46409
T [K]	293(2)	100(2)	45(2)	26(2)	50(2)
	dark	dark	dark	light	dark
$\theta_{min}-\theta_{max}$	2.23–29.25	2.26–29.05	1.53–18.00	1.53–16.86	1.67–18.01
scan type	ω	ω	ϕ	ϕ	ϕ
limiting indices					
	$-14 > h > 18$	$-13 > h > 17$	$-16 > h > 16$	$-16 > h > 16$	$-16 > h > 16$
	$-14 > k > 6$	$-13 > k > 13$	$-13 > k > 13$	$-12 > k > 12$	$-13 > k > 13$
	$-24 > l > 24$	$-24 > l > 23$	$-23 > l > 22$	$-21 > l > 21$	$-23 > l > 17$
total reflections collected	10151	14 130	12603	14511	8468
indep refl	3205	3074	2762	2354	2611
R_{int}	0.0361	0.0383	0.0399	0.0891	0.0556
refl with $I > 2\sigma(I)$	2207	2521	2307	1823	2003
absorption correction	0.79/0.94	0.77/0.94	0.88/0.97	0.91/0.95	0.89/0.96
refinement					
data/restrains/parameters	3205/0/159	3074/0/159	2762/0/159	2354/134/159	2611/140/159
final R indices [$I > 2\sigma(I)$]					
$R1$	0.0427	0.0330	0.0338	0.0414	0.0519
$wR2$	0.1037	0.0735	0.0894	0.0929	0.1157
final R indices (all data)					
$R1$	0.0716	0.0461	0.0436	0.0563	0.0730
$wR2$	0.1163	0.0784	0.0956	0.1021	0.1237
GoF on F^2	1.006	1.074	1.056	1.067	1.045
final (Δ/σ)max	0.000	0.000	0.000	0.000	0.000
largest diff. peak and hole [e Å^{-3}]	0.587/ – 0.707	0.712/ – 0.680	0.617/ – 1.240	1.209/ – 1.183	1.945/ – 1.387

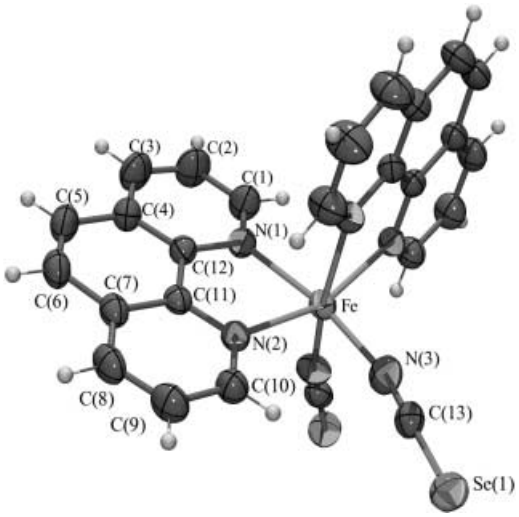

Figure 3. Molecular structure of high-spin $[Fe(phen)_2(NCSe)_2]$ (**HS-1**) at 293 K showing the atom numbering scheme.

crystalline sample in this work, we expect this data to be of very high quality, and much more representative of the individual spin states.

Structure of high-spin [Fe(phen)$_2$(NCSe)$_2$] at 298 K (HS-1): The iron local coordination geometry in the room temperature high-spin state (Figure 3) is based on a distorted octahedron, with Fe–N(CSe) bond lengths of 2.080(3) Å, and Fe–N(phen) bond lengths of 2.187(2) and 2.188(2) Å (see Table 2). These Fe–N bond lengths result in significant distortion from octahedral geometry, with the largest being observed for the ligand bite angle (N(1)-Fe-N(2)) of 75.77(9)°, the 102.55(10)° angle between *cis* phen and NCSe ligands (N(2a)-Fe-N(3)) and the 160.92(12)° angle between the *trans* nitrogen atoms of the phen ligands (N(2)-Fe-N(2a)). The angle between the NCSe and *trans* N of the phen ligands (N(3)-Fe-N(1)) is 166.23(10)°. Guionneau et al.[37] have recently recommended the use of the distortion parameter, Σ (defined as the sum of the absolute values of the deviation from 90° of the 12 *cis* angles within the coordination sphere[38]) for the study of iron(II) spin crossover compounds. For **HS-1**, a value of 61.1° is obtained, which is very close to that observed for high-spin $[Fe(phen)_2(NCS)_2]$.[15] The RMS deviation from planarity of the phen groups is 0.0217 Å with the largest deviation being found for C(2) and N(1) (one above, the other below), with the iron atom 0.104 Å out of the plane in the same direction as N1, and the angle between the planes of the two phen ligands is 86.33°. [All the atoms in the phen ligand were used with the following equation: $0.2243(0.0073)x+6.9658(0.0043)y+12.8838(0.0068)z=5.4729(0.0021)$.] The NCSe units are approximately linear (178.8(3)°), and the Fe-N-C(Se) bond angles are 165.6(3)°. The Se sits in a pocket of H atoms from the phen ligands from the neighbouring molecules. The Fe-N-C(Se) linkage seems fairly flexible as bond angles from 130 to 171° have been observed in the previous four single crystal X-ray studies of iron(II) compounds with NCSe ligands.[39]

Table 2. Bond lengths [Å] and angles [°] for the iron coordination environment in $[Fe(phen)_2(NCSe)_2]$.

	HS-1	LS-1a	LS-1b	HS-2	LS-2
Fe–N(1)	2.187(2)	1.971(2)	1.978(2)	2.197(3)	1.987(4)
Fe–N(2)	2.188(2)	1.992(2)	1.997(2)	2.202(3)	2.003(3)
Fe–N(3)	2.080(3)	1.933(2)	1.937(2)	2.095(3)	1.943(4)
N(3)–C(13)	1.146(4)	1.153(3)	1.151(3)	1.164(5)	1.155(6)
C(13)–Se(1)	1.785(3)	1.796(2)	1.806(3)	1.799(4)	1.809(5)
N(1)-Fe-N(2)	75.77(9)	82.36(8)	82.33(9)	75.81(12)	82.27(15)
N(1a)-Fe-N(2a)	75.77(9)	82.36(8)	82.33(9)	75.81(12)	82.27(15)
N(1)-Fe-N(1a)	89.81(14)	92.31(11)	92.35(13)	89.25(16)	92.3(2)
N(1)-Fe-N(2a)	90.63(9)	92.38(8)	92.16(9)	89.28(12)	92.03(15)
N(1a)-Fe-N(2)	90.63(9)	92.38(8)	92.16(9)	89.28(12)	92.03(15)
N(1)-Fe-N(3a)	89.58(10)	89.19(8)	89.07(9)	90.10(12)	89.08(16)
N(1a)-Fe-N(3)	89.58(10)	89.19(8)	89.07(9)	90.10(12)	89.08(16)
N(2)-Fe-N(3)	90.48(10)	90.87(8)	90.90(9)	89.86(12)	90.88(15)
N(2a)-Fe-N(3a)	90.48(10)	90.87(8)	90.90(9)	89.86(12)	90.88(15)
N(2)-Fe-N(3a)	102.55(10)	94.48(8)	94.71(8)	104.44(12)	94.89(14)
N(2a)-Fe-N(3)	102.55(10)	94.48(8)	94.71(8)	104.44(12)	94.89(14)
N(3)-Fe-N(3a)	94.25(16)	90.11(12)	90.30(13)	94.02(18)	90.4(2)
N(2)-Fe-N(2a)	160.92(12)	172.43(11)	172.06(13)	159.14(17)	171.81(18)
N(1)-Fe-N(3)	166.23(10)	173.12(8)	173.12(9)	165.66(12)	173.07(15)
N(1a)-Fe-N(3a)	166.23(10)	173.12(8)	173.12(9)	165.66(12)	173.07(15)
Fe-N(3)-C(13)	165.6(3)	165.45(19)	165.0(2)	164.1(3)	165.0(3)
N(3)-C(13)-Se(1)	178.8(3)	178.2(2)	178.6(2)	178.8(3)	178.4(4)

The molecular packing (Figure 4) is best described as sheets of complexes in the *ab* plane with the essentially planar phen ligands forming a herring-bone pattern alternating in direction between the sheets in the *c* direction. The shortest

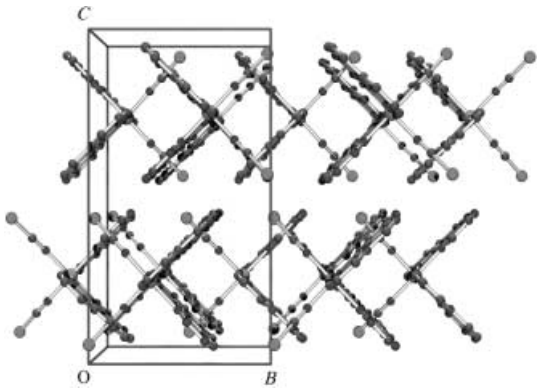

Figure 4. Molecular packing diagram of high-spin $[Fe(phen)_2(NCSe)_2]$ (**HS-1**) in the *bc* plane. (Hydrogen atoms omitted for clarity).

intermolecular contacts (less than the sum of the van der Waals radii[40]) (see Table 3) all involve the NCSe ligand and are 3.359 Å between Se(1) and C(6), 2.761 Å between C(13) and H(8), and 3.096 Å between Se(1) and H(1). The short Se(1)–C(6) intermolecular interaction results in a 2D network (see Figure 5) extending in the *ac* plane, and inclusion of the C(13)–H(8) contacts results in a 3D network. The nonbonding contact interactions between the carbon atoms of the phen ligands are all in excess of the sum of the van der Waals radii, and up until 0.4 Å greater than this all of the contacts are within the sheets.

Structure of low-spin [Fe(phen)$_2$(NCSe)$_2$] at 100 K (LS-1a): The space group at 100 K is the same as at 298 K, and the reduction in unit cell volume from 2376 to 2261 Å^3 is a result of a reduction in the *a*, *b* and *c* dimensions of 0.401, 0.045 and

Table 3. Shortest intermolecular contacts [Å] in $[Fe(phen)_2(NCSe)_2]$.[a]

	Sum of van der Waals radii[b]	HS-1	LS-1a	LS-1b	HS-2	LS-2
Se(1)−C(6) $3	3.60	3.359	3.363	3.341	3.249	3.341
Se(1)−C(5) $3	3.60	3.622	3.738	3.716	3.492	3.718
Se(1)−H(1) $1	3.10	3.096	3.050	3.037	3.067	3.044
Se(1)−H(3) $2	3.10	3.175	3.098	3.088	3.128	3.102
Se(1)−H(5) $2	3.10	3.175	3.164	3.145	3.077	3.148
Se(1)−H(6) $3	3.10	3.178	3.077	3.064	3.117	3.062
C(13)−H(8) $5	2.90	2.761	2.705	2.701	2.748	2.704
C(13)−H(6) $5	2.90	3.098	2.888	2.877	3.104	2.897
C(13)−H(3) $2	2.90	2.969	2.884	2.863	2.861	2.876
N(3)−H(8) $5	2.75	2.808	3.030	3.004	2.635	3.008

[a] $3 etc. indicate intermolecular contacts with different molecules in the unit cell. [b] van der Waals radii:[40] C 1.70 Å, H 1.20 Å, N 1.55 Å, Se 1.90 Å.

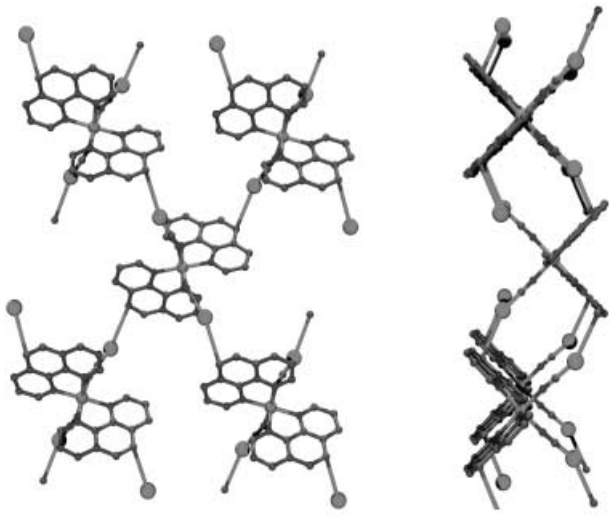

Figure 5. 2D-network of short intermolecular contacts between Se(1) and C(6) in the *ac* plane (left) and the *bc* plane (right) of low-spin $[Fe(phen)_2(NCSe)_2]$ (**LS-1b**) (Hydrogen atoms omitted for clarity).

0.255 Å, respectively. These reductions are greater than would be expected from thermal effects alone. There is very little change in the angle between the planes of the two phen ligands (87.65°) and the phen ligands are still essentially planar with a RMS deviation of 0.0262 Å and the largest deviation being found for N(1), C(2) and C(3), with N(1) lying below the plane and C(2) and C(3) above the plane. The iron atom has also moved slightly more out of the plane (0.138 Å) than in **HS-1**, in the same direction as N1. [All the atoms n the phen ligand were used with the following equation: $-0.4912(0.0051)x+7.0205(0.0033)y+12.5445(0.0056)z=5.5126\ (0.0016)$.] The Fe-N-C(Se) bond angle (165.45°) remains essentially the same as does the linearity of the N-C-Se unit (178.2°). The changes in the cell dimensions are due to a shortening of all of the Fe–N bonds. The Fe–N(CSe) bond lengths shorten by 0.147 to 1.933(2) Å, whereas the Fe–N(-phen) bond lengths have shortened by 0.216 and 0.196 Å to 1.971(2) (Fe–N(1)) and 1.992(2) Å (Fe–N(2)), respectively. The largest changes are observed for the Fe–N(phen) bonds *trans* to the NCSe ligands, indicating that phen is a better π-acceptor ligand than NCSe. The reduction in the Fe–N bond lengths also causes a change in the iron coordination environment; this results in a much more regular octahedron, and this is reflected in a large reduction in the Σ distortion parameter to only 34.8°. These changes are shown in Figure 6.

The reduction in bond lengths and close approach to a regular octahedral geometry is common for iron(II) spin crossover compounds on going from high-spin to low-spin,[36] and is usually explained by an increase in the π-backbonding expected for the low-spin isomers. It is generally assumed that phen is a better π acceptor ligand than NCSe, and therefore these bond lengths show a greater reduction when going from high- to low-spin, as observed above. If the Fe–N bond lengths are shortened by an increase in back-donation to the ligands, then it is also to be expected that other bonds will also be affected, and as the donation is into π* antibonding orbitals on either the phen or NCSe ligands a slight increase in these bond lengths is anticipated. In the earlier crystallographic study[28] of $[Fe(phen)_2(NCS)_2]$, no significant changes were observed in the phen interatomic distances but a decrease of 0.018 Å in the N–C(S) bond length and a small increase in the S–C bond length of 0.014 Å in the thiocyanate ligands was observed on cooling from 293 to 130 K. In contrast, in this work there is a very small increase on cooling in both the N–C(Se) (1.146 to 1.153 Å) and C–Se (1.785 to 1.796 Å) bond lengths in the NCSe ligands, and changes of this order have also been observed in $[Fe(bipy)_2(NCS)_2]$.[41] In addition to these changes, small increases in most of the interatomic distances in the phen ligands (see Table 4) were also observed. Whilst most of these differences are small, the fact that the data was collected from the same crystal in sequential data sets and that the majority of the differences are in the same direction, leads us to believe that they are probably a genuine reflection of the difference in back-bonding between the two spin states. The packing is essentially the same in **HS-1** and **LS-1a**, but there are some slight differences in the Se–H distances and coordination environment. The three closest intermolecular contacts (in terms of van der Waals radii) (Table 3) in the low-spin structure are 3.363 Å (Se(1)–C(6)), 2.705 Å (C(13)–H(8)) and 3.050 Å (Se(1)–H(1)) which are longer, shorter and shorter, respectively, than their high-spin counterparts. In the low-spin structure there are now a total of seven short contacts less than the sum of the van der Waals radii compared to three for the high-spin structure, and all of

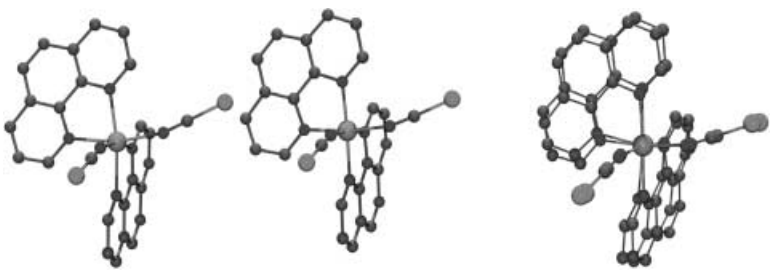

Figure 6. Comparison of the molecular structures of $[Fe(phen)_2(NCSe)_2]$ in its high-spin (**HS-1**) (left), and low-spin (**LS-1a**) (centre) states, and the two structures superimposed (right). (Hydrogen atoms omitted for clarity).

Table 4. Bond lengths [Å] within the 1,10-phenanthroline ligands in $[Fe(phen)_2(NCSe)_2]$.

	HS-1	LS-1a	LS-1b	HS-2	LS-2
N(1)–C(1)	1.316(4)	1.333(3)	1.333(3)	1.329(5)	1.338(6)
N(1)–C(12)	1.358(4)	1.366(3)	1.367(3)	1.367(5)	1.376(5)
N(2)–C(10)	1.332(4)	1.336(3)	1.335(3)	1.332(5)	1.341(5)
N(2)–C(11)	1.356(3)	1.362(3)	1.363(3)	1.365(5)	1.366(6)
C(11)–C(12)	1.433(4)	1.423(3)	1.427(3)	1.444(5)	1.432(6)
C(1)–C(2)	1.393(4)	1.402(3)	1.404(4)	1.411(5)	1.395(6)
C(4)–C(12)	1.402(4)	1.398(3)	1.401(3)	1.406(5)	1.393(6)
C(7)–C(11)	1.405(4)	1.406(3)	1.406(3)	1.411(5)	1.413(6)
C(9)–C(10)	1.379(5)	1.396(3)	1.405(3)	1.394(5)	1.406(6)
C(2)–C(3)	1.359(5)	1.366(4)	1.371(4)	1.372(6)	1.372(6)
C(3)–C(4)	1.390(5)	1.407(3)	1.414(3)	1.422(5)	1.421(6)
C(4)–C(5)	1.427(5)	1.429(3)	1.438(4)	1.437(5)	1.443(6)
C(5)–C(6)	1.354(5)	1.355(4)	1.363(4)	1.364(5)	1.367(6)
C(6)–C(7)	1.430(4)	1.437(3)	1.437(4)	1.447(5)	1.436(6)
C(7)–C(8)	1.392(5)	1.405(3)	1.415(3)	1.408(6)	1.416(6)
C(8)–C(9)	1.366(5)	1.374(3)	1.375(4)	1.388(6)	1.379(6)

these involve the NCSe ligand. Whilst it is interesting and often instructive to identify the small variations in the intermolecular interactions between the spin states in order to understand the cooperativity, it is important to remember that after a very detailed crystallographic study of the spin transitions in a number of iron(II) complexes Guionneau et al. came to the conclusion that it is "…the whole topology of the interaction which has to be taken into account…".[36]

The differences in the Fe–N bond lengths observed between the high-spin (**HS-1**) and low-spin (**LS-1**) states in this work are larger than those observed previously for $[Fe(phen)_2(NCS)_2]$ using either single crystal diffraction[15, 28, 29] or EXAFS.[12, 42] This is most likely to be due to the fact that the crystals of $[Fe(phen)_2(NCSe)_2]$ were grown using the extraction method, whereas the diffusion method was used for $[Fe(phen)_2(NCS)_2]$, and from the magnetic susceptibility data it is clear that the sample of $[Fe(phen)_2(NCSe)_2]$ used in this work undergoes an essentially complete spin transition, whereas there is around 16% of the high-spin form still present in the low-spin state of $[Fe(phen)_2(NCS)_2]$. Therefore, we believe that our data is the most accurate available for the structural changes associated with the spin transition in $[Fe(phen)_2(NCS)_2]$ or $[Fe(phen)_2(NCSe)_2]$ complexes. [In one report, the Fe–N bond length differences derived from single crystal experiments on $[Fe(phen)_2(NCSe)_2]$ were more similar to those observed herein, but no details were reported for the data acquisition and refinement at 300 K.[12]]

Structure of the LIESST induced metastable high-spin state of $[Fe(phen)_2(NCSe)_2]$ (HS-2): In order to provide a direct comparison of the structural changes occurring during the LIESST process we tried to record data for the room temperature high-spin state of $[Fe(phen)_2(NCSe)_2]$ (**HS-1**) at the ESRF, but this was not possible due to radiation damage problems. However, data for the low temperature, low-spin state (**LS-1**) were recorded at ≈50 K, both before (**LS-1b**) and after (**LS-2**) the visible irradiation. (It was not possible to use 100 K for these data due to technical constraints of the cryostats.) The initial work on the structure of the LIESST induced metastable high-spin state, **HS-2**, made use of an Oxford Cryosystems Helix cryostat (combined closed cycle and He flow gas) at the ESRF. Whilst the structure of the **LS-1** state determined from these experiments was essentially identical to that obtained from the Daresbury data, only very small changes in the cell volume, lattice parameters and Fe–N bond lengths were observed after irradiation at ≈35–40 K, and these were well below the values anticipated from the previous EXAFS experiments.[12] (The single crystal data[15] on the $[Fe(phen)_2(NCS)_2]$ **HS-2** structure had not been submitted or published at this time.) This non-observation of a structural change upon irradiation at low temperature is thought to have arisen from a combination of two effects: i) the sample not being sufficiently cold for a significant proportion of the **HS-2** state to be stabilized as the Helix cryostat has a formal base temperature of ≈30–40 K, and the alignment of the sample within the cold zone is very critical; and ii) the fact that the crystals are very deeply coloured, and that it is seems necessary to use crystals that are not totally opaque. Therefore, on a subsequent occasion at ID11 of the ESRF the smallest crystals possible were used together with an Oxford Diffraction HeliJet cryostat (liquid He and He flow gas cryostat) which has a formal base temperature of <15 K, and a much larger cold zone. The experiments described below all made use of this equipment, although the base temperature was limited to ≈25 K.

The data collected from the low-spin state at 100 K at Daresbury (**LS-1a**) and at 45 K at the ESRF (**LS-1b**) are essentially identical (see Figure 7a, Tables 3 and 4) with cell volumes of 2260.8 and 2254.4 Å^3, respectively. All of the Fe–N bond lengths are within 3.5σ, which is very acceptable given that the data were collected at two different synchrotron sources using different wavelengths. The data at 45 K was collected in the dark to reduce the extent of ambient light induced LIESST. In order to avoid shattering the crystal when irradiated below the LIESST critical temperature, the sample was illuminated and rotated during cooldown from 45 to 26 K, and was kept illuminated throughout the data collection (**HS-2**). Even with these precautions, broadening of the diffraction peaks indicated some strain in the crystal due to several significant structural modifications. At 26 K, when bathed in visible light the cell volume expanded by 73 Å^3 (3.3%) from

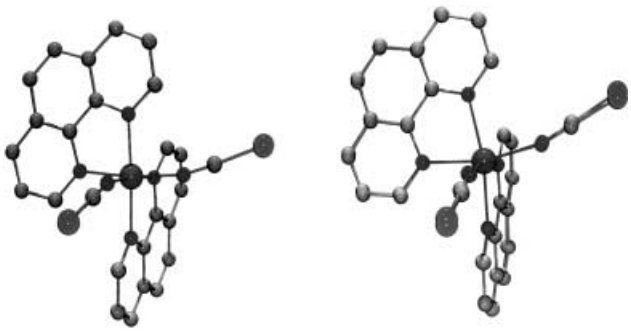

Figure 7. Comparison of the low-spin structures (superposition of **LS-1a**, **LS-1b**, **LS-2**) of $[Fe(phen)_2(NCSe)_2]$ (left), and comparison of the high-spin structures (superposition of **HS-1** and **HS-2**) of $[Fe(phen)_2(NCSe)_2]$ (right) (Hydrogen atoms omitted for clarity).

2254.4 to 2327.0 Å^3, compared with a cell volume for **HS-1** of 2376.3 Å^3. Some reduction of the cell volume is to be expected between **HS-1** and **HS-2** due to lower thermal motion. As to be expected from these data both the lattice parameters and the Fe–N bond lengths for **HS-1** and **HS-2** are also are very similar. It should be noted that in the previous work on the **HS-2** state of $[Fe(phen)_2(NCS)_2]$,[15] the increase in cell volume for the **LS-1** to **HS-2** conversion was only 24 Å^3, although the difference between the cell volumes of **HS-1** and **LS-1** of $[Fe(phen)_2(NCS)_2]$ at 119 Å^3 is comparable to that for $[Fe(phen)_2(NCSe)_2]$ at 115 Å^3. As noted earlier we attribute these discrepancies to the higher quality crystal/sample available for the $[Fe(phen)_2(NCSe)_2]$ work. The Fe–N bond lengths are all slightly longer in **HS-2** compared to **HS-1**, but the differences between Fe–N(phen) bond lengths in **HS-1** and **LS-1a**, and in **LS-1b** and **HS-2** are probably not very significant. However, the differences between the Fe–N(CSe) bond lengths in **HS-1** (2.080(3) Å) and **HS-2** (2.095(3) Å) appear to be more significant, and this correlates with an increase of 0.018 Å in N(3)–C(13) on going from **LS-1b** to **HS-2**, whereas a reduction of the order of 0.007 Å would be expected from the **HS-1** to **LS-1a** transition. The change in the C(13)–Se(1) bond length is slightly smaller, but of the expected sign between **LS-1b** and **HS-2**. The changes in the bond lengths in the phenthroline ligands are probably not significant. A comparison of the **HS-2** and **HS-1** structures is shown in Figure 7b, where the difference in the NCSe unit can be seen clearly. The behaviour of the NCSe ligand in **HS-2** also has a strong effect on the non-bonded intermolecular contacts. For example in **HS-2** as compared to **LS-1b** the Se(1)–C(6) and Se(1)–C(5) interactions decrease by 0.09 and 0.22 Å, respectively, and the N(3)–H(8) interaction reduces by 0.369 Å. These interactions are also 0.11, 0.13 and 0.17 Å shorter in **HS-2** than **HS-1**. Therefore, whilst it is clear that the structure of **HS-2** in terms of Fe–N bond lengths and N-Fe-N bond angles (with a Σ value of 64.0°) is very similar to that of **HS-1**, there are some subtle, and probably very important differences between the high-spin structures which can give insight into the cooperativity that must be present in the solid state. It should be remembered that there were also small but significant differences in the IR spectra of **HS-2** and **HS-1**. All the shortest intermolecular contacts involve the NCSe ligand in all cases. In the previous report[15] on the **HS-2** structure of $[Fe(phen)_2(NCS)_2]$ a similar observation regarding the Se(1)–C(6) non-bonded interactions was made. However, some of their conclusions regarding the cooperativity mechanism may need to be re-assessed, as these were based on a much smaller cell volume change, possibly due to incomplete conversion either due to the temperature or the need for optically transparent crystals.

In order to demonstrate the reversibility of the LIESST process (reverse-LIESST is not possible with $[Fe(phen)_2(NCS)_2]$ or $[Fe(phen)_2(NCS)_2]$ due to the overlap of the electronic absorption bands[25, 33, 34]) the same crystal was warmed to 50 K in the dark and a data set was obtained for **LS-2**. The cell volume reduced to 2270.8 Å^3 compared with 2327.0 Å^3 for **HS-2** and 2254.4 Å^3 for **LS-1b**. The Σ parameter returned to 35.6°, and all of the Fe–N bond lengths are within 2σ of those for **LS-1b**. The new, short, non-bonded interactions that appeared in **HS-2** reverted to their original values in **LS-1b**. Therefore, the structure of **LS-1b** and **LS-2** can be regarded as identical, indicating the complete structural reversibility of the photochemical process. The structural similarity of the **LS-1a**, **LS-1b** and **LS-2** structures is clearly demonstrated in Figure 7a where all three are superimposed on top of each other.

Conclusion

This work has provided the first structural data for $[Fe(phen)_2(NCSe)_2]$ in its high-spin (**HS-1**) or low-spin (**LS-1**) states, and because of the quality of the sample and the crystals we believe that this data contains the best example of structural changes occurring upon spin crossover in iron(II) phenanthroline complexes. In addition, the first structural data from the LIESST induced metastable high-spin state (**HS-2**) of $[Fe(phen)_2(NCSe)_2]$ at $\approx$26 K has been reported. These data show that whilst the structures of **HS-1** and **HS-2** are very similar there appear to be a number of significant differences involving the NCSe ligand. In all spin states the shortest intermolecular contacts involve the NCSe ligand, which may be of relevance to understanding the cooperativity that facilitates the abrupt spin transitions. The structure of the **LS-2** low-spin state that forms when **HS-2** is allowed to warm to $\approx$50 K has also been obtained, and this demonstrates that the process is completely reversible as the structures of the low-spin states before (**LS-1b**) and after (**LS-2**) LIESST are essentially identical.

Experimental Section

Synthesis: The synthesis and characterization of $[Fe(phen)_2(NCSe)_2]$ by Soxhlet extraction of $[Fe(phen)_3](NCSe)_2$ using pyridine under nitrogen for 2 d has been described in detail elsewhere.[9]

Physical measurements: The LIESST experiments were carried out using a tungsten lamp and fibre guide to eliminate thermal effects at the sample. The variable temperature magnetic susceptibility measurements were made using a Quantum Design Physical Property Measurement System (PPMS) operating at 1.0 T. The variable temperature IR spectra were recorded using a Bruker Equinox55 FTIR spectrometer, with the samples in the form of pressed KBr discs mounted on the cold station of an APD DE204 closed cycle cryostat within a vacuum chamber.

X-ray crystallographic measurements: **HS-1** and **LS-1a** were collected on station 9.8[43] at the Daresbury Laboratory Synchrotron Radiation Source (SRS), using a Bruker SMART 1K CCD area detector diffractometer and silicon monochromated radiation ($\lambda = 0.6878$ Å) at 293 and 100 K, respectively. **LS-1b**, **HS-2** and **LS-2** were collected at station ID11 of the European Synchrotron Radiation Facility (ESRF) on a Bruker SMART 6500 CCD system using silicon monochromated radiation ($\lambda = 0.46409$ Å) at 45 K (dark), 26 K (light), 50 K (dark), respectively. SAINT[44] was used to integrate the data sets and apply the Lorentz and polarisation corrections. Crystal data and details of the data collection and refinement are given in Table 1. SADABS[45] was used to apply the absorption correction to all data and the incident beam decay correction for SRS data. The incident beam decay correction for ESRF data was provided by a feedback system on the monochromator. The structures were solved by direct methods using SHELXS-97.[46] The structures were refined on F^2 using full-matrix least squares (SHELXL-97).[47] For all data sets all non-hydrogen atoms were refined with anisotopic displacement parameters. H atoms were placed geometrically and refined by riding models with $U_{iso}(H) = 1.2U_{eq}(C)$. The largest peaks and holes in the difference maps are around the heavy atoms.

Neutral atom scattering factors were taken from the International Tables for Crystallography[48] and anomalous dispersion corrections were calculated using CROSSEC.[49]

CCDC-203747 (**HS-1**), -203745 (**LS-1a**), -203746 (**LS-1b**), -203749 (**HS-2**), -203748 (**LS-2**) contain the supplementary crystallographic data for this paper. These data can be obtained free of charge via www.ccdc.cam.ac.uk/conts/retrieving.html (or from the Cambridge Crystallographic Data Centre, 12 Union Road, Cambridge CB2 1EZ, UK; (fax: (+44) 1223-336-033; or e-mail: deposit@ccdc.cam.ac.uk).

Acknowledgement

We gratefully acknowledge the support of the EPSRC for equipment, personnel (C.M.McG. and F.E.S.) and SRS beamtime (GR/K 64662), a post-graduate studentship (J.M.W.S.) and access to the EPSRC Chemical Database Service at Daresbury Laboratory;[50] DARPA funding for AMRI (MDA972-97-1-0003); the Director of the Synchrotron Radiation Division at Daresbury Laboratory and the Director General of the ESRF for access to synchrotron and computing facilities.

[1] a) E. König, *Coord. Chem. Rev.* **1968**, *3*, 471; b) H. A. Goodwin, *Coord. Chem. Rev.* **1976**, *18*, 293; c) E. König, G. Ritter, S. K. Kulshreshtha, *Chem. Rev.* **1985**, *85*, 219; d) M. Bacci, *Coord. Chem. Rev.* **1988**, *86*, 245; e) E. König, *Prog. Inorg. Chem.* **1987**, *35*, 527; f) H. Toftlund, *Coord. Chem. Rev.* **1989**, *94*, 67; g) E. König, *Struct. Bonding* **1991**, *76*, 51; h) A. Hauser, J. Jeftić, H. Romstedt, R. Hinek, H. Spiering, *Coord. Chem. Rev.* **1999**, *190–192*, 471; i) H. Spiering, T. Kohlhaas, N. Romstedt, A. Hauser, C. Bruns-Yilmaz, J. Kusz, P. Gütlich, *Coord. Chem. Rev.* **1999**, *190–192*, 629; j) J. A. Real, A. B. Gaspar, V. Niel, M. C. Muñoz, *Coord. Chem. Rev.* **2003**, *236*, 121.

[2] P. Gütlich, Y. Garcia, H. A. Goodwin, *Chem. Soc. Rev.* **2000**, *29*, 419.

[3] E. König, K. Madeja, *Chem. Commun.* **1966**, 61.

[4] a) S. Decurtins, P. Gütlich, C. P. Köhler, H. Spiering, A. Hauser, *Chem. Phys. Lett.* **1984**, *105*, 1; b) S. Decurtins, P. Gütlich, K. M. Hasselbach, A. Hauser, H. Spiering, *Inorg. Chem.* **1985**, *24*, 2174; c) S. Decurtins, P. Gütlich, C. P. Köhler, H. Spiering, *J. Chem. Soc. Chem. Commun.* **1985**, 430.

[5] P. Gütlich, A. Hauser, H. Spiering, *Angew. Chem.* **1994**, *106*, 2109; *Angew. Chem. Int. Ed. Engl.* **1994**, *33*, 2024.

[6] P. Gütlich, Y. Garcia, T. Woike, *Coord. Chem. Rev.* **2001**, *219–221*, 839.

[7] a) C. J. O'Connor, E. Sinn, T. J. Bucelot, B. S. Deaver, *Chem. Phys. Lett.* **1980**, *74*, 27; b) A. W. Addison, S. Burman, C. G. Wahlgren, O. A. Rajan, T. M. Rowe, E. Sinn, *J. Chem. Soc. Dalton Trans.* **1987**, 2621.

[8] a) P. Gütlich, J. Ensling, F. Tuczek, *Hyperfine Interact.* **1994**, *84*, 447; b) P. Gütlich, *Mol. Cryst. Liqd. Cryst. A* **1997**, *305*, 17.

[9] D. Collison, C. D. Garner, C. M. McGrath, J. F. W. Mosselmans, M. D. Roper, J. M. W. Seddon, E. Sinn, N. A. Young, *J. Chem. Soc. Dalton Trans.* **1997**, 4371.

[10] a) J. Zarembowitch, O. Kahn, *New J. Chem.* **1991**, *15*, 181; b) O. Kahn, J. Krober, C. Jay, *Adv. Mater.* **1992**, *4*, 718; c) C. Jay, F. Groliere, O. Kahn, J. Krober, *Mol. Cryst. Liqd. Cryst. A* **1993**, *234*, 255; d) P. Gütlich, *Nucl. Instrum. Methods Phys. Res. Sect. B* **1993**, *76*, 387; e) O. Kahn, *Curr. Opin. Solid State Mater. Sci.* **1996**, *1*, 547; f) O. Kahn, E. Codjovi, Y. Garcia, P. J. Vankoningsbruggen, R. Lapouyade, L. Sommier, *ACS Symp. Ser.* **1996**, *644*, 298; g) O. Kahn, E. Codjovi, *Philos. Trans. R. Soc. London A* **1996**, *354*, 359; h) O. Kahn, C. J. Martinez, *Science* **1998**, *279*, 44; i) O. Kahn, *Chem. Br.* **1999**, *35*, 24; j) J. B. Gaudry, L. Capes, P. Langot, S. Marcen, M. Kollmannsberger, O. Lavastre, E. Freysz, J. F. Létard, O. Kahn, *Chem. Phys. Lett.* **2000**, *324*, 321; k) Y. Garcia, V. Ksenofontov, P. Gütlich, *Hyperfine Interact.* **2002**, *139*, 543.

[11] L. X. Chen, Z. Wang, J. K. Burdett, P. A. Montano, J. R. Norris, *J. Phys. Chem.* **1995**, *99*, 7958.

[12] J. J. Lee, H. S. Sheu, C. R. Lee, J. M. Chen, J. F. Lee, C. C. Wang, C. H. Huang, Y. Wang, *J. Am. Chem. Soc.* **2000**, *122*, 5742.

[13] J. Kusz, H. Spiering, P. Gütlich, *J. Appl. Crystallogr.* **2000**, *33*, 201.

[14] J. Kusz, H. Spiering, P. Gütlich, *J. Appl. Crystallogr.* **2001**, *34*, 229.

[15] M. Marchivie, P. Guionneau, J. A. K. Howard, G. Chastanet, J. F. Létard, A. E. Goeta, D. Chasseau, *J. Am. Chem. Soc.* **2002**, *124*, 194.

[16] V. A. Money, I. R. Evans, M. A. Halcrow, A. E. Goeta, J. A. K. Howard, *Chem. Commun.* **2003**, 158.

[17] a) E. König, *Coord. Chem. Rev.* **1968**, *3*, 471; b) P. Gütlich, *Struct. Bonding* **1981**, *44*, 83.

[18] W. A. Baker, H. M. Bobonich, *Inorg. Chem.* **1964**, *3*, 1184.

[19] E. König, K. Madeja, *Inorg. Chem.* **1967**, *6*, 48.

[20] K. F. Purcell, M. P. Edwards, *Inorg. Chem.* **1984**, *23*, 2620.

[21] J. Pebler, *Inorg. Chem.* **1983**, *22*, 4125.

[22] E. König, K. Madeja, *Spectrochim. Acta A* **1967**, *23*, 45.

[23] J. H. Takemoto, B. Hutchinson, *Inorg. Chem.* **1973**, *12*, 705.

[24] M. Sorai, S. Seki, *J. Phys. Chem. Solids* **1974**, *35*, 555.

[25] R. H. Herber, *Inorg. Chem.* **1987**, *26*, 173.

[26] B. Maiti, B. R. McGarvey, P. S. Rao, L. C. Stubbs, *J. Magn. Reson.* **1983**, *54*, 99.

[27] P. Ganguli, P. Gütlich, E. W. Müller, W. Irler, *J. Chem. Soc. Dalton Trans.* **1981**, 441.

[28] B. Gallois, J. A. Real, C. Hauw, J. Zarembowitch, *Inorg. Chem.* **1990**, *29*, 1152.

[29] J. A. Real, B. Gallois, T. Granier, F. Suezpanama, J. Zarembowitch, *Inorg. Chem.* **1992**, *31*, 4972.

[30] T. Granier, B. Gallois, J. Gaultier, J. A. Real, J. Zarembowitch, *Inorg. Chem.* **1993**, *32*, 5305.

[31] E. W. Müller, H. Spiering, P. Gütlich, *Chem. Phys. Lett.* **1982**, *93*, 567.

[32] C. M. McGrath, C. J. O'Connor, C. Sangregorio, J. M. W. Seddon, E. Sinn, F. E. Sowrey, N. A. Young, *Inorg. Chem. Commun.* **1999**, *2*, 536.

[33] R. Herber, L. M. Casson, *Inorg. Chem.* **1986**, *25*, 847.

[34] K. U. Baldenius, A. K. Campen, H. D. Hohnk, A. J. Rest, *J. Mol. Struct.* **1987**, *157*, 295.

[35] a) G. Brehm, M. Reiher, S. Schneider, *J. Phys. Chem. A* **2002**, *106*, 12024; b) M. Reiher, *Inorg. Chem.* **2002**, *41*, 6928.

[36] P. Guionneau, J. F. Létard, D. S. Yufit, D. Chasseau, G. Bravic, A. E. Goeta, J. A. K. Howard, O. Kahn, *J. Mater. Chem.* **1999**, *9*, 985.

[37] P. Guionneau, C. Brigouleix, Y. Barrans, A. E. Goeta, J. F. Létard, J. A. K. Howard, J. Gaultier, D. Chasseau, *C.R. Chim.* **2001**, *4*, 161.

[38] a) F. A. Deeney, C. J. Harding, G. G. Morgan, V. McKee, J. Nelson, S. J. Teat, W. Clegg, *J. Chem. Soc. Dalton Trans.* **1998**, 1837; b) M. G. B. Drew, C. J. Harding, V. McKee, G. G. Morgan, J. Nelson, *J. Chem. Soc. Chem. Commun.* **1995**, 1035.

[39] a) A. Ozarowski, Y. Shunzhong, B. R. McGarvey, A. Mislankar, J. E. Drake, *Inorg. Chem.* **1991**, *30*, 3167; b) T. J. Mizoguchi, S. J. Lippard, *Inorg. Chem.* **1997**, *36*, 4526; c) N. Moliner, M. C. Muñoz, S. Létard, J. F. Létard, X. Solans, R. Burriel, M. Castro, O. Kahn, J. A. Real, *Inorg. Chim. Acta* **1999**, *291*, 279; d) N. Moliner, M. C. Muñoz, J. A. Real, *Inorg. Chem. Commun.* **1999**, *2*, 25.

[40] A. Bondi, *J. Phys. Chem.* **1964**, *68*, 441.

[41] E. König, K. J. Watson, *Chem. Phys. Lett.* **1970**, *6*, 457.

[42] G. Sankar, J. M. Thomas, V. Varma, G. U. Kulkarni, C. N. R. Rao, *Chem. Phys. Lett.* **1996**, *251*, 79.

[43] a) R. J. Cernik, W. Clegg, C. R. A. Catlow, G. Bushnell-Wye, J. V. Flaherty, G. N. Greaves, I. Burrows, D. J. Taylor, S. J. Teat, M. Hamichi, *J. Synchr. Radiat.* **1997**, *4*, 279; b) W. Clegg, M. R. J. Elsegood, S. J. Teat, C. Redshaw, V. C. Gibson, *J. Chem. Soc. Dalton Trans.* **1998**, 3037.

[44] *SMART and SAINT*, Area-Detector Control and Integration Software, Bruker, Madison, WI (USA), **1997**.

[45] G. M. Sheldrick, *SADABS*, Program for Scaling and Correction of Area Detector Data, University of Göttingen, **1997**.

[46] G. M. Sheldrick, *SHELXS-97*, Program for the Solution of Crystal Structures, University of Göttingen, **1997**.

[47] G. M. Sheldrick, *SHELXL-97*, Program for the Refinement of Crystal Structures, University of Göttingen, **1997**.

[48] J. E. Wilson, *International Tables for Crystallography*, *Vol. C*, **1992**, Kluwer, Dordrecht.

[49] a) D. T. Cromer, *J. Appl. Crystallogr.* **1983**, *16*, 437; b) S. Bailey, *Acta Crystallogr. Sect. D Biol. Crystallogr.* **1994**, *50*, 760.

[50] D. A. Fletcher, R. F. McMeeking, D. Parkin, *J. Chem. Inf. Comput. Sci.* **1996**, *36*, 746.

Received: February 20, 2003
Revised: May 12, 2003 [F4865]

